

Electrochemical and Microstructural Analysis of Azomethine Polyamides as Inhibitor for Rebar Corrosion under Chloride Contaminated Pore Solution

Bhuvaneshwari Balasubramaniam^{1*}, Athiramu Selvaraj², Nagesh R. Iyer³, Lingam Ravikumar², Prabhat K. Rai⁴, K. Mondal⁴, Raju Kumar Gupta^{1,5*}

¹Department of Chemical Engineering, Indian Institute of Technology Kanpur, Kanpur 208016, Uttar Pradesh, India

²Department of Chemistry, C.B.M College, Bharathiar University, Coimbatore 641042, Tamil Nadu, India

³Department of Mechanical Engineering, Indian Institute of Technology, Dharwad, Karnataka 580011, India

⁴Department of Materials Science and Engineering, Indian Institute of Technology Kanpur, Kanpur 208016, Uttar Pradesh, India

⁵Center for Environmental Science and Engineering, Indian Institute of Technology Kanpur, Kanpur 208016, Uttar Pradesh, India

*Corresponding Author. Email: B. Bhuvaneshwari, bhuvib@iitk.ac.in; Raju Kumar Gupta, guptark@iitk.ac.in

Received: 04 December 2018, Accepted: 18 December 2018, Published Online: 20 December 2018

Citation Information: Bhuvaneshwari Balasubramaniam, Athiramu Selvaraj, Nagesh R Iyer, Lingam Ravikumar, Prabhat K Rai, K Mondal, Raju Kumar Gupta. *Frontier Research Today* 2018;1:01004. doi: 10.31716/frt.201801004 Cite in Other Styles

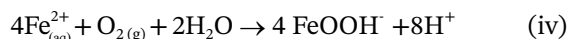
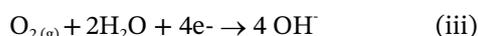
ABSTRACT: The present study deals with the synthesis of two structurally different azomethine polyamides and their effect as inhibitor for a steel rebar in chloride containing pore solution. The amorphous and crystalline natures of the polymers were evaluated based on the XRD analysis. Potentiodynamic polarisation and impedance spectroscopy were employed to investigate the inhibition efficiency of the polymers for the protection of the rebar during corrosion. Scanning electron microscopic and atomic force microscopic techniques were used for the surface characterization of the steel in presence of the adsorbed layer formed by the polymer molecule leading to the inhibition from corrosion. The adsorption of the polyamide inhibitors on the steel rebar obeyed Langmuir adsorption isotherm. Two polyamide inhibitors showed similar inhibition efficiency at concentration ranging from 10 to 1000 ppm and maximum efficiency of 99.62% was achieved by the polymer PAMA1. Formation of protective layer on the surface of steel rebar by the inhibitors was attributed to be the reason for corrosion protection under chloride contaminated pore solution.

Keywords: Azomethine Polyamides; Corrosion; Rebar; Electrochemistry

1 INTRODUCTION

The corrosion of rebar steel imposes a major impact on the economics of construction industry for meeting the cost of repair and rehabilitation. In general, the cost of corrosion is expected to be ~2.5 trillion US dollars per year worldwide with respect to the global economy¹. It is an issue of prime importance where the structure is prone to corrosion and bring economic burden and imposes safety threat to the environment².

In general, corrosion process involves the oxidation of metals and charge balance is maintained by the reduction of oxygen or protons (H⁺), or water depending on the pH and presence of active species for reduction. Corrosion process of steel in presence of oxygen or water is presented by the following reactions^{3,4}



There could be possibility of hydrogen reduction reaction (H⁺ + e⁻ = 0.5 H₂) as well as water reduction (2H₂O + 2e⁻ = H₂ + 2OH⁻).

Since corrosion is a thermodynamically feasible process, it is difficult to stop the corrosion completely, rather

it needs to be controlled or minimized. There are several techniques for corrosion protection or control to a permissible limit⁵⁻⁷. Some of the widely used techniques are

- (i) choice of proper material,
- (ii) use of coating, removal of the corrosives like O₂, halides, moisture, proper design of components,
- (iii) electrochemical protection methods such as sacrificial anode, self-healing coatings, advanced treatment processes, impressed current cathodic protection or forcing passivation of the metal and use of inhibitors,^{1,8,9}
- (iv) application of inhibitor.^{8,10,11}

A state-of-the-art report has been published on corrosion inhibitors for steel rebar in concrete¹⁰, covering the entire spectrum of commonly used inhibitors, such as amino alcohols, calcium nitrite and sodium monofluoro phosphates. The important discussions made in the review articles are mainly on

- (a) understanding the inhibition mechanism of inhibitors,
- (b) inhibitors efficiency for the corrosion of steel rebar in most vulnerable chloride rich environments and with carbonated concrete,
- (c) difficulties faced by the penetrability of the migrating corrosion inhibitors (MCIs) during penetration into concrete when applied,
- (d) inhibitors influence on fresh state and hardened state properties of concrete and their function in mechanical performances of concrete and effects durability, and

(e) real time monitoring like field trials considering availability of limited data at present on the long-term performance of the inhibitors and their functions in real structures.

Also important aspects of using corrosion inhibitors for the protection of steel rebar from corrosion at vulnerable environmental conditions were emphasized in detail in recent literatures¹⁰⁻¹⁶.

Although inorganic based corrosion inhibitors, mainly nitrite^{17,18}, and other organic based corrosion inhibitors¹⁹⁻²⁴ are used for the corrosion protection of rebar, their negative impact on setting time and strength reduction are yet to be studied in detail^{10,25}. ShaoBo Jiang et al.^{15,26,27} reported the carcinogenic nature and biological toxicity of nitrite and nitrate based inorganic inhibitors and hence, their usage was banned in many countries. Hence emergence arrives on finding an alternate to the above said inhibitors. Recently, polymer based corrosion inhibitors are gaining more attention due to their extraordinary performance in providing corrosion protection for metals, such as steel, aluminum and copper²⁸⁻³⁷. Currently, extensive research focusses on the usage of intrinsic conductive polymers (ICPs) as corrosion inhibitor⁴ for the protection of rebar from corrosion in spite of difficulty faced during their production.

Solubility is also an issue with the industrial solvent. Further, recent studies on the polymer based inhibitors for protection of steel rebar from corrosion in the simulated chloride contaminated environment have proven their merit^{8,31,38,39} as anti-corrosive agent. However, only limited data are available on the polymer based corrosion inhibitors for the protection of rebar under corrosion. In addition, there is lack of clear understanding on the corrosion inhibition mechanism of the polymeric inhibitors. Bhuvaneshwari et al.⁸ have synthesized the azomethine based polyesters and employed them as corrosion inhibitor for the protection of rebar from corrosion. It was concluded in their study that 98% inhibition efficiency was achieved at 1000 ppm of azomethine polyester during the corrosion of rebar in the simulated and chloride ions contaminated concrete pore solution. It was also mentioned in their study that the polymers have high potential to function as effective inhibitor even at low concentrations for the corrosion protection of rebar. Chan Basha Nusrath Unnisa et al.³⁹ used the polyesters namely Poly (Glycerol azealate) (PGAZ) and 4-(1-(4-methoxy phenyl) cyclo hexyl) phenyl 9-oxo-decanoate (MPOD), as a corrosion inhibitor for corrosion protection of rebar in simulated chloride contaminated concrete environment. The maximum inhibition efficiency of 71.8% was achieved with the MPOD inhibitors and minimum of 57.6% was achieved with the PGAZ.

However, to the best of author's knowledge in this particular area, there are not many investigations available in open literature on the use of polymeric based inhibitors for protecting steel rebar from chloride induced corrosion except a few as mentioned above^{8,30,38}. In the present study, synthesis of two functional polymers with amide linkage has been carried out and their inhibition efficiency for the protection of rebar from corrosion in chloride contaminated pore solution has been investigated by two potentiodynamic polarization and electrochemical impedance spectroscopy.

2 EXPERIMENTAL DETAILS

2.1 Chemicals used

4,4' - diamino diphenyl ether, 4,4' - diamino diphenyl methane, Ammonium thiocyanate, 4- amino benzoic acid, Terephthaldehyde, p-Toluene sulphonic acid, Ethanol, Hydrochloric acid, Triphenyl phosphorite, Calcium chloride, Sodium carbonate, Pyridine, Chloroform, Potassium hydroxide, *N*-Methyl-2-pyrrolidone (NMP), *N,N'*-dimethylformamide (DMF) were used for the synthesis of azomethine polyamides. All the solvents were purified before start of the experiments. All chemicals involved in the synthesis were of AR grade and were purchased from M/s Merck India Pvt Ltd.

2.2 Synthesis of azomethine polyamides

The two azomethine polyamides used namely azomethine polyamide 1 (PAMA1) and azomethine polyamide 2 (PAMA2) were synthesized by following the synthesis procedure developed by Ravikumar et al.⁴⁰ The synthesis method mainly involves three stages such as (i) synthesis of dicarboxylic acid monomers having azomethine group (ii) synthesis of phenyl thiourea diamine monomer and (iii) synthesis of polyamide by phosphorylation condensation of two monomers.

For the synthesis of dicarboxylic acid monomers having azomethine group, a clean 50 mL round bottomed flask equipped with a reflux condenser, Dean-Stark trap and a magnetic stirrer were used. It was then charged with 0.2 mole of 4-aminobenzoic acid, 0.01 mole of terephthaldehyde and 30 mL of absolute ethanol and catalytic quantities of p-toluene sulphonic acid. At room temperature itself the reaction mixture was stirred for 15 min after that heated in an oil bath at 110 °C. An azeotrope was formed, and it was collected in the Dean-Stark trap apparatus. The further refluxing of the as obtained contents was carried out for 45-60 min and then about 10 mL of ethanol was distilled off. The remaining slurry was again refluxed for 3 h. At the end, a precipitate collected were cooled, filtered and washed several times with hot water. Then the resultant products were finally washed with absolute ethanol and dried under vacuum. In next step synthesis of phenyl thiourea diamine monomer was carried out separately⁴¹.

Finally, to synthesis the azomethine polymers, phosphorylation condensation method was employed. A mixture of 0.004 mole of the dicarboxylic acid monomer, 0.04 mole of diamino diphenyl methane monomer, 0.01 mole of triphenyl phosphorite, 1.2 g of dry CaCl₂, 4 mL of pyridine and 10 mL of NMP was heated in a round bottom flask with stirring at 110 °C for 4-5 h. A viscous liquid of the polymer was formed due to condensation process. After that the polymer was thrown out in the form of a precipitate by pouring the viscous liquid into 300 mL of absolute ethanol with continuous stirring. Then the polymers obtained was filtered, washed several times with hot water, and washed with dilute Na₂CO₃ solution, dilute HCl and hot water, in succession. The resultant polymers were finally washed with absolute ethanol and dried under vacuum. The viscosity measurements of the as-synthesized polymers were conducted in DMF medium. The polymerisation process or the

synthesis scheme of the synthesized polymers are shown in **Figure 1**.

2.3 Characterisation of polymers

X-ray diffraction (XRD) studies were carried out on the as synthesized polymers with the help of D2 Phaser Desktop model of Bruker XRD instrument equipped with Ni-filtered Cu α radiation (30kV accelerating voltage and 10mA emission current). The data collected over the 2θ range of 0° to 70° by keeping the step size of 0.0017 and a scan rate of $7^\circ/\text{min}$. The percentage crystallinity ($\%X_c$) of the as synthesized polymers PAMA1 and PAMA2 were calculated from the XRD data.

2.4 Electrochemical investigations

The rebar used in the present study consisted of Mn-0.69, Si-0.26, Cr-0.176, C-0.15, Ni- 0.13, Cu-0.115, W - 0.08, Mo-0.06 S- 0.039, P- 0.026, Co- 0.02, Ti -0.02, Nb-0.01, B-0.0007, V-0.006, Al- 0.004, and rest Fe- 98.22 (all in wt%).

In order to assess the inhibition efficiency and the corrosion rate of the polymers PAMA1 and PAMA2 towards steel rebar corrosion in simulated chloride contaminated pore solution, potentiodynamic polarisation and impedance spectroscopy were employed. The flat corrosion cell consisted of a reference electrode namely saturated calomel electrode, a working electrode (steel rebar) with 1 cm^2 working area and a platinum counter electrode with working area slightly more than the working electrode. Saturated calomel electrode ($E^0 = 0.241\text{V}$ with reference to standard hydrogen electrode) was used as reference electrode and the luggin capillary was inserted near to the working electrode. The simulated pore solution contaminated with chloride ions having the ratio of 0.5 M KOH + 0.1 M NaOH +0.5 M

NaCl was used as electrolyte (pH around 8.5-9). Hereafter, the simulated chloride contaminated pore solution would be referred as blank. Prior to start the experiment, working electrode was grounded with 220, 320, 400, 600, 800, 1000, 1200, 1500 grade silicon carbide emery papers and then micro polishing was done with $0.5\ \mu\text{m}$ - $1.0\ \mu\text{m}$ diamond paste and degreasing with acetone and distilled water, then finally cleaned ultrasonically. The as-prepared polymers were added in ppm level, such as 10 ppm, 100 ppm and 1000 ppm into the test solution individually during polarization of the steel rebar. All the tests were performed at room temperature ($\sim 298\text{ K}$).

2.4.1 Polarization studies

Prior to the start of experiment, open circuit potential (OCP) values were stabilized by immersing the sample for 3600 s to reach the steady state condition. After getting stabilized OCP, linear and potentiodynamic polarizations of steel rebar were carried out using Metrohm Autolab (POTENTIOSTAT 100 workstation) in freely aerated electrolyte i.e blank solution with and without inhibitors. Polarization resistance (R_p) has been obtained by calculating the slope of the linear polarization plot at zero over-potential given by the equation (v) according to ASTM standard G102-89.⁴²

$$\text{Polarization resistance } (R_p) = (\Delta E/\Delta i) \quad (v)$$

Potentiodynamic polarization tests were also performed at the scan rate of 0.166 mV/s at room temperature. The corrosion current density (i_{corr}) was determined using the Tafel extrapolation method. In the present investigation, potentiodynamic polarization measurements have been carried out to evaluate the inhibition efficiency of the inhibitors for steel rebar in as prepared blank solution. The inhibitor efficiency (η) was calculated from the following equation:

$$\eta\% = (i_{\text{corr}}^0 - i_{\text{corr}}/i_{\text{corr}}^0) \times 100 \quad (vi)$$

where, i_{corr}^0 and i_{corr} are corrosion current densities of steel rebar in blank and inhibited solution respectively.

2.4.2 Impedance studies

To investigate the overall corrosion behavior and the interfacial structure of steel-pore solution, electrochemical impedance spectroscopy (EIS) was performed for the steel samples exposed to the pore solutions with different types of polymeric inhibitors of varying concentrations. Electrochemical impedance spectroscopy (EIS) studies were conducted by applying a sinusoidal potential perturbation of 10 mV at stabilized OCP in the frequency range of 100 kHz to 10 mHz in blank solution with and without the inhibitors. Obtained data points were modelled using Metrohm Autolab Nova software (version 1.9) and fitted with the help of equivalent electrical circuit as shown in the inset of **Figure 4** (a). Among the various AC techniques, Faradaic impedance method is widely adopted as this technique facilitates the determination of double layer capacitance and charge transfer resistance. From the plot Z'' versus Z' (Nyquist plot), charge transfer resistance (R_{ct}) value has been determined. Further, the C_{dl} values have been obtained from the

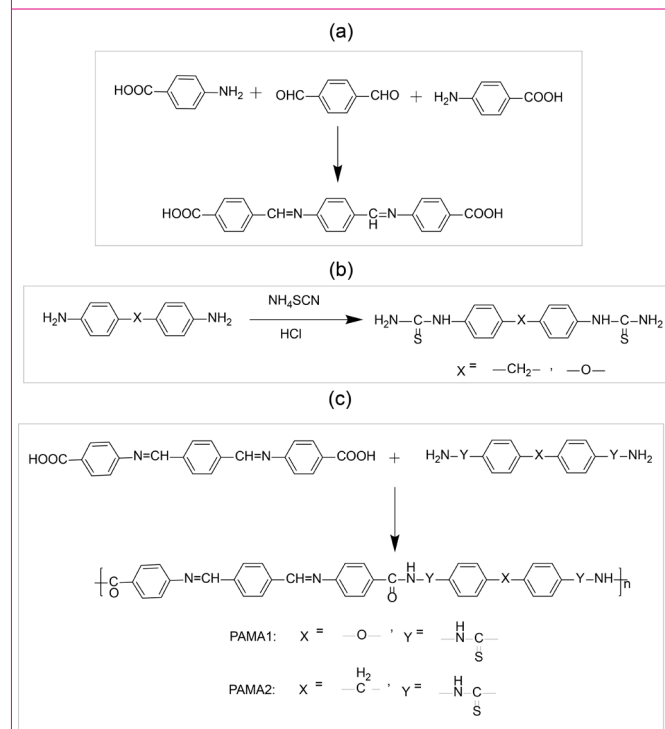


Figure 1. Synthesis scheme of polymers a) synthesis scheme for azomethine dicarboxylic acid monomer b) synthesis scheme for phenyl thiourea diamine monomer c) synthesis scheme for azomethine polyamides.

following equation

$$F(-Z''_{\max}) = 1/(2\pi C_{dl} R_{ct}) \quad (vi)$$

2.5 Microstructure

The morphology of the polished steel rebar, steel rebar exposed to blank solution and in the presence of PAMA1 and PAMA2 inhibitors (1000 ppm) during corrosion was examined by scanning electron microscopy (SEM). This study would be helpful to assess the surface coverage role played by the polymeric inhibitors for the protection of rebar from corrosion. The SEM images were taken with the help of scanning electron microscope model Tescan Vega-3 with the accelerating voltage of 30 kV. Surface topography analysis of steel rebar after polishing and in the presence of polymer PAMA2 was conducted using atomic force microscopy (AFM). The non-contact mode AFM images were taken using the atomic force microscope XE-70 PARK SYSTEM.

3 RESULTS AND DISCUSSION

The structure of the polymers, PAMA1 and PAMA2, are shown in Table 1. The viscosities of the azomethine polymers, PAMA1 and PAMA2, are found to be 0.63 and 0.59, respectively.

3.1 XRD characterization of polymers

The XRD spectrum of the PAMA1 and PAMA2 are shown in Figure 2. The calculated % crystallinity ($\%X_c$) of the PAMA1 is ~ 61% and 39% amorphous and the PAMA2 consists of 86% crystalline and 14% amorphous. The dual phase (crystalline and amorphous) nature of the polymers is indicative of the solid state complex characteristics of the synthesized polymers. The physical properties, such as structure, color and yield of the polymers PAMA1 and PAMA2, are also presented in Table 1.

3.2 Electrochemical analysis of polymers

The polarisation plots obtained for the steel rebar exposed to blank solution in presence and absence of the PAMA1 and the PAMA2 are shown in Figure 3 (a and b).

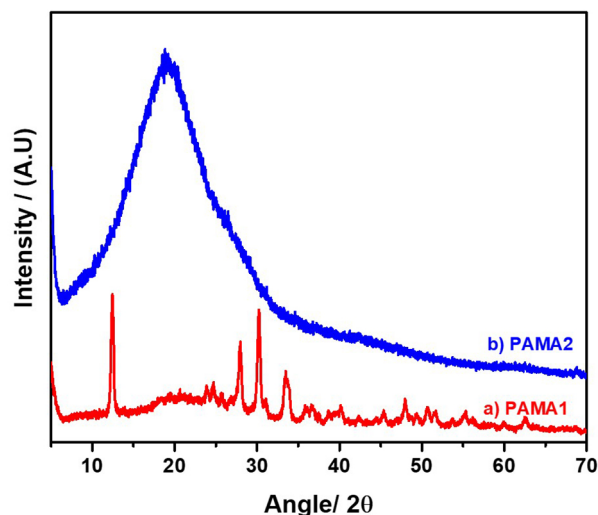


Figure 2. XRD spectrum of PAMA1 and PAMA2.

The corresponding electrochemical parameters, such as corrosion potential (E_{corr}), corrosion current (I_{corr}), β_c , β_a and corrosion rate (CR), as computed from the potentiodynamic polarisation studies are shown in Table 2. From the polarisation data, it is understood that the highest inhibition efficiency (η) of 99.62% is achieved by the 1000 ppm of inhibitor PAMA1 for the corrosion protection of the rebar in chloride contaminated pore solution. Interestingly, the two polymeric inhibitors, viz., PAMA1 and PAMA2 show an excellent corrosion inhibition efficiency at 10 ppm itself. In particular, the inhibitor efficiency of the PAMA2 beyond 10 ppm follows the same trend up to 1000 ppm as indicated in Table 2.

The impedance spectra obtained for the steel rebar exposed to blank solution in presence and absence of the PAMA1 and the PAMA2 are shown in Figure 4 (a and b) and the corresponding calculated impedance parameters, such as R_{ct} and C_{dl} , values are shown in Table 2. The analysis of impedance plots reveals that the rebar steel – electrolyte interface response shows only one loop as capacitive arcs. The characteristics of impedance spectra for the rebar in blank and in the presence of azomethine polyamide inhibitors are following similar trend as seen in their corresponding figures. The simple Randle circuit is used to fit the impedance data (insets in Figure 4 (a, b)), where R_s in-

Table 1. Physical characterization of the PAMA1 and PAMA2

Sl. No.	Structure of the compounds	Color	Yield (%)
1	<p style="text-align: center;">PAMA1</p> <p style="text-align: center;">Polyazomethine amide 1</p>	Dirty White	92
2	<p style="text-align: center;">PAMA2</p> <p style="text-align: center;">Polyazomethine amide 2</p>	Dirty White	90

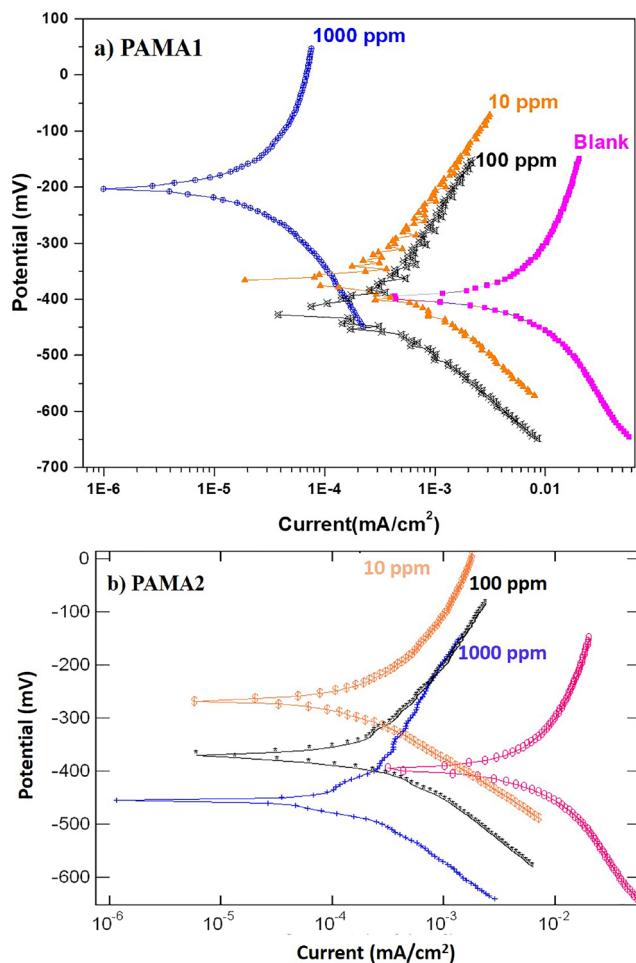


Figure 3. Polarization plots of a) PAMA1 and b) PAMA2.

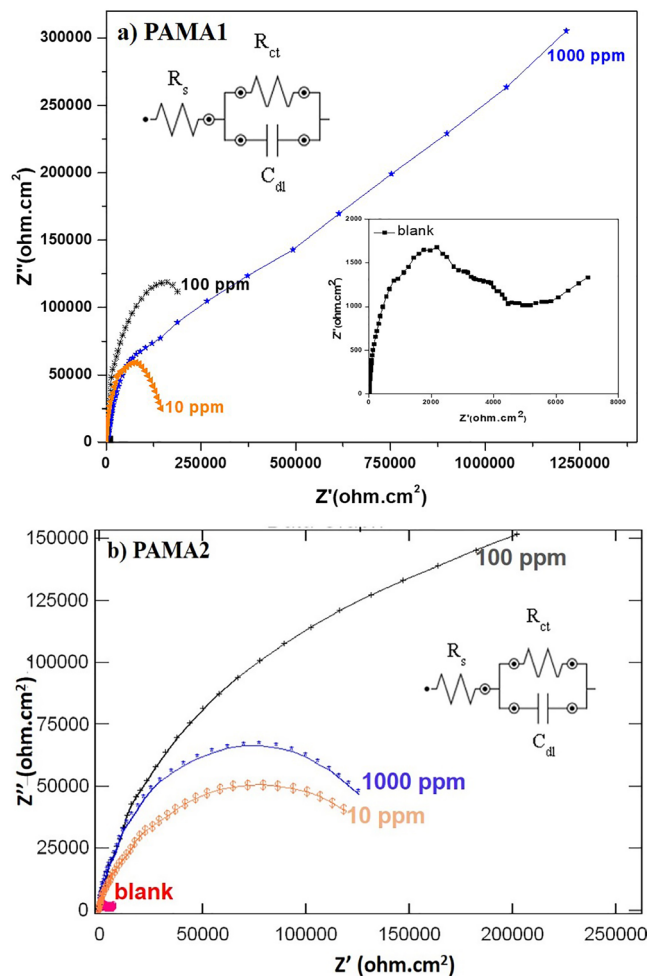


Figure 4. Nyquist plots of a) PAMA1 and b) PAMA2.

Table 2. Electrochemical parameters of PAMA1 and PAMA2

PAMA1								
Inhibitor conc. (ppm)	E_{corr} (-mV)	I_{corr} ($\mu\text{A}/\text{cm}^2$)	B_a (mV/dec)	B_c (mV/dec)	R_{ct} (Ohms/ cm^2)	C_{dl} ($\mu\text{F}/\text{cm}^2$)	IE (η) (%)	Corrosion Rate (mm/year)
Simulated pore solution with Cl-	396.89	5.3	350.31	195.07	0.3661	34.86	-	0.0883
10	370.45	0.22	229.95	91.62	12.44	23.05	95.84	0.0044
100	418.23	0.21	191.49	123.27	27.61	26.18	96.03	0.0048
1000	204.26	0.02	314.36	187.70	39.94	48.52	99.62	0.00034
PAMA2								
10	269.05	0.15	168.03	131.40	12.84	30.28	97.16	0.0035
100	370.90	0.13	154.75	92.67	16.05	27.14	97.54	0.0030
1000	455.45	0.12	193.61	122.30	30.21	26.08	97.73	0.0019

indicates the solution resistance and the nanometric adsorptive film resistance contributed by the polymeric inhibitors, R_{ct} , indicates the charge transfer resistance and C_{dl} refers the double layer capacitance.

As the Nyquist plots are not perfect semicircles, the difference attributes to the frequency dispersion^{43, 44}. It is important to notice that the radii of the semi-circles mainly depend on the additive or inhibitor concentrations. The results show that the R_{ct} value increases with increasing

polymers concentration, supports the formation of surface film with increasing concentration. Also, increase in R_{ct} and decrease in C_{dl} with increase in polymer concentration during corrosion of rebar refer the higher surface coverage facilitated by the inhibitor. Further, the protection efficiencies of polymers during the rebar corrosion confirms the interaction role played by the polymeric functional groups with the active sites of the steel rebar.

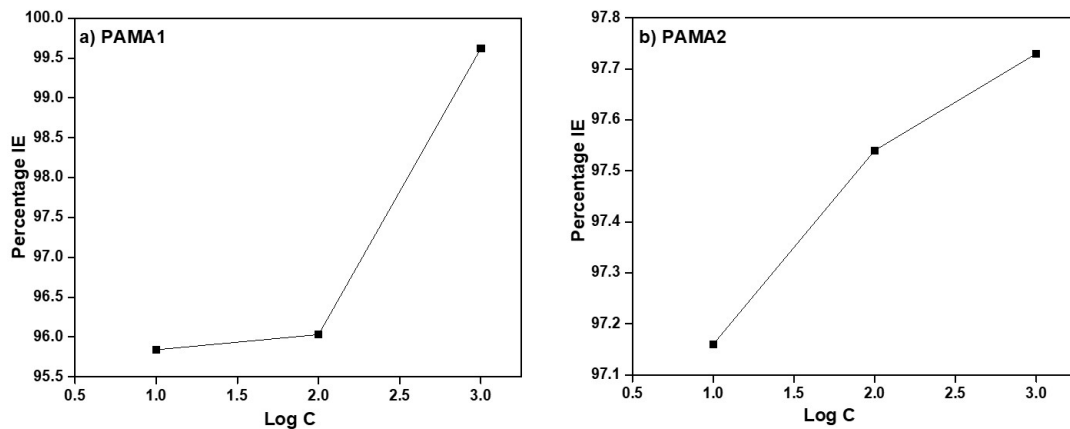


Figure 5. Log C vs % IE of a) PAMA1 and b) PAMA2.

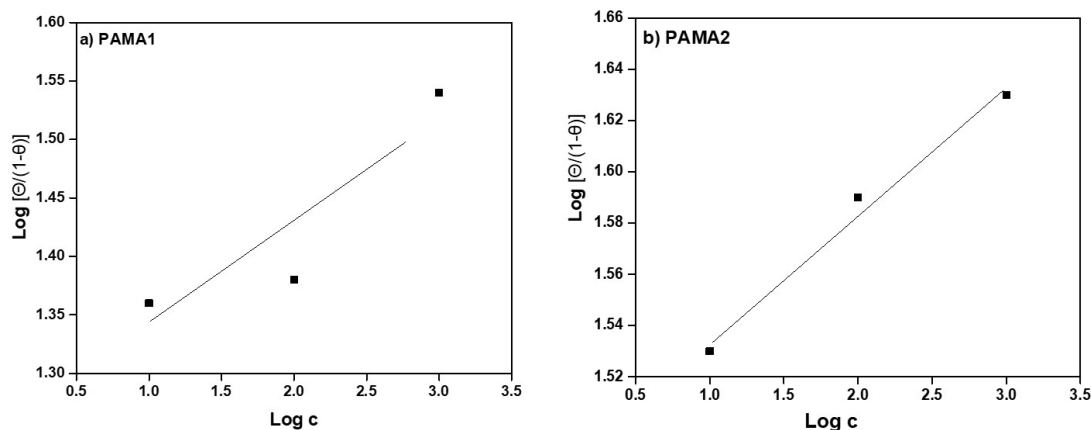


Figure 6. Adsorption Isotherm of a) PAMA1 and b) PAMA2.

3.3 Surface coverage of inhibitors and their inhibitor efficiency and related adsorption isotherm

The surface coverages of the PAMA1 and PAMA2 with respect to the corresponding inhibitor efficiency on the steel rebar during the corrosion in chloride contaminated pore solution are plotted in **Figure 5** (a, b). The variation of inhibition efficiency as a function of inhibitor concentrations is shown. The corresponding adsorption isotherms are constructed by using surface coverage values as shown in **Figure 6** (a, b). This provides the basic information about the surface interaction of the metal with the inhibitor molecules. This would help in arriving adsorption mechanism of the polymer molecules and their nature. The famous approach as accepted by majority is that adsorption of organic molecules follow mainly two types of adsorption i.e chemisorption (or physisorption). Analysis of these plots reveals that the azomethine polyamides in chloride contaminated pore solutions follow the Langmuir adsorption. Since adsorption isotherms follows Langmuir type, the organic molecule attached to the metal surface as a monolayer by physisorption. However, sometimes electron density in the polymers also responsible for the interaction with metal surface and hence this can be argued that at a given situation or response, the polymers would have adsorbed on metal surface via chemisorption as well. It is well reported that chemisorption involves charge sharing or charge

transfer from the inhibitor molecules to the metal surface which resulted in the formation of a coordinate-type bond⁴⁵ thereby uniform and high surface coverage occurs. The mechanism of adsorption of polymers on steel rebar surface during corrosion is elaborated in section 3.6.

3.4 Characterization of corrosion products using SEM

Figure 7 (a-d) show the SEM images of the polished steel rebar, steel rebar exposed to blank and in presence of 1000 ppm of PAMA1 and PAMA2 inhibitors as obtained after polarization experiment. The microstructure of the polished rebar specimen has no pit holes or cavities which ensures the surface uniformity of the specimen after polishing. However, the presence of cavities in the microstructure of rebar exposed to blank solution as shown in **Figure 7** (b) confirms the corrosion effect by Cl⁻ ions. The SEM images as shown in **Figure 7** (c and d) show the existence of highly dense and uniform protective layer over the steel surfaces. The results indicate that the presence of inhibitors in pore solution has an auto-repairing effect on the defective areas of adsorptive layer during the corrosion of rebar under vulnerable environment. There is also a possible scenario that the protective film might have been formed due to the formation of complex between the corrosion products and the solution components of chlorides and inhibitors, which have protected the metal from further attack. However,

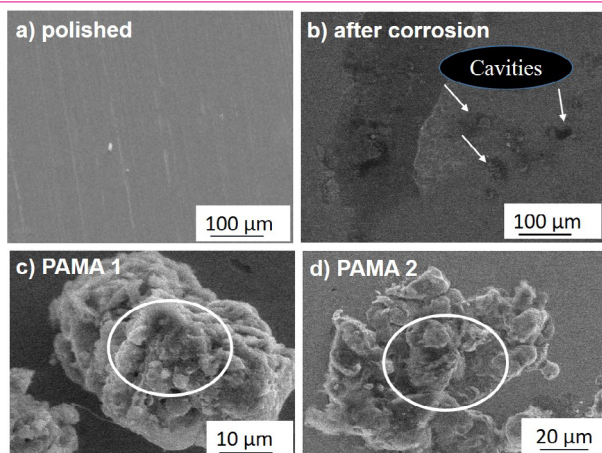


Figure 7. SEM micrograph of a) polished steel rebar b) steel rebar after corrosion in blank c) steel rebar after corrosion in presence of PAMA1 d) steel rebar after corrosion in presence of PAMA2.

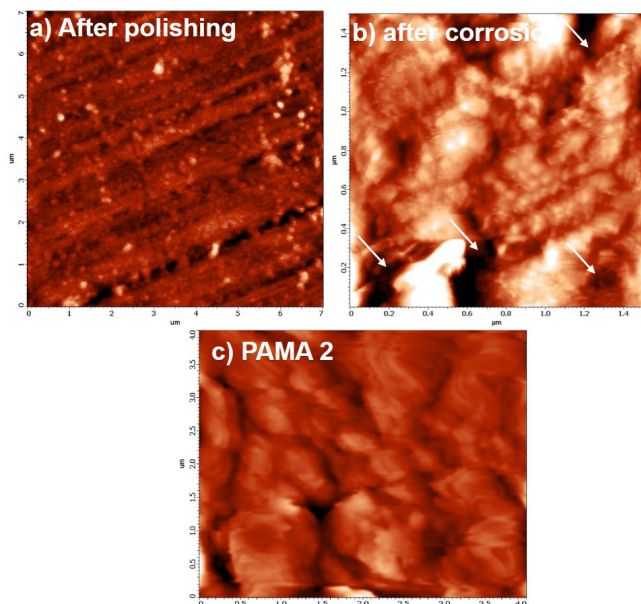


Figure 8. AFM topography of a) polished steel rebar b) steel rebar after corrosion in blank c) steel rebar after corrosion in presence of PAMA2.

component levels studies are required to prove that mechanism, which can also be helpful in understanding the long term performance of the inhibitors on strength and durability of aspects the concrete structures.

3.5 AFM surface analysis of rebar steel

AFM was used to probe the surface of steel rebar in the presence and absence of adsorbed polymer film. The 2D topography image of the plain steel rebar after polishing and the steel rebar after corrosion in the presence of the blank and the PAMA2 inhibitor are shown in **Figure 8** (a-c), respectively. As seen in **Figure 8** (a), the polished rebar shows no corrosion pit. However, a distinct topographies are seen in the AFM images of the rebar in the presence of the blank and the inhibitor PAMA2. Pit holes due to the corrosion attack by Cl^- ions on the steel rebar surface in the absence of inhibitors are clearly visible in **Figure 8** (b). It is evident from this study that the addition of the PAMA2

changes the topography of the steel rebar through film adsorption on its surface. Hence, the AFM result of the rebar in presence of the PAMA2 during corrosion process indicates that the as-formed protective layer contributes to the protection of the steel rebar against chloride attack in the simulated pore solution.

3.6 Mechanism of inhibition by azomethine polyamides

It is well known that the interface inhibition between metal/solution mainly depends on the nature and charge of the metal, the chemical resonance or structure of the inhibitor, functional group, aromaticity, electronic structure of inhibitors and the type of electrolyte used^{8, 39}. The bonding of the inhibitor molecules on the surface of metal is mainly influenced by the functional group present in it^{8, 39}. It is a well-known phenomenon that more is the functional or branches in the structure, higher would be the adsorption of inhibitor resulting in higher inhibition. In the present study, the expected mechanism of the PAMA1 and the PAMA2 as inhibitors is found to be mainly due to:

- i. Displacement of Cl^- ions and water molecules from the rebar steel surface by the polyamide molecules.
- ii. Formation of a gel like adduct between the displaced Cl^- ions and polymer molecules.
- iii. Formation of coordination type of complex between Fe^{2+} ions on metal surface and the gel leading to strong adsorptions, which may be both chemisorption and physisorption and thereby rendering metal surface hydrophobic.
- iv. Prevention of the ingress of both the aggressive Cl^- ions as well as water molecules towards the metal surface.
- v. During the adsorption, the aromatic polyamide molecules orient themselves in near flat orientation with reference to the metal surface. The aromatic rings, azomethine groups $-\text{CH}=\text{N}-$, $-\text{C}=\text{S}$ and $-\text{CONH}$, act as anchoring sites with their rich electron density.
- vi. The polymer molecules arrange themselves parallel to each other on the metal surface forming an organic monolayer that covers the entire metal surface and effectively block the ingress of Cl^- ions.

The general adsorption behavior of aromatic polymer on the metal surface during chloride induced corrosion is represented in **Figure 9** (a). Further, the adsorption nature of individual polymer molecules such as PAMA1 and PAMA2 on the steel surface during corrosion can be depicted as shown in **Figure 9** (b, c). The results also emphasized that the orientation of the molecules, nature of each functional groups interactions and their electron donating and withdrawing nature with respect to time dependent exchange process etc have made the as synthesized functional polymers as unique and frontier inhibitor for the protection of steel rebar from corrosion⁸.

4 CONCLUSIONS

The above studies conclude that the two azomethine polyamides, namely PAMA1 and PAMA2, were successfully synthesized and they act as novel inhibitor for the corrosion protection of the steel rebar from corrosion in chloride contaminated pore solution. The maximum efficiency of

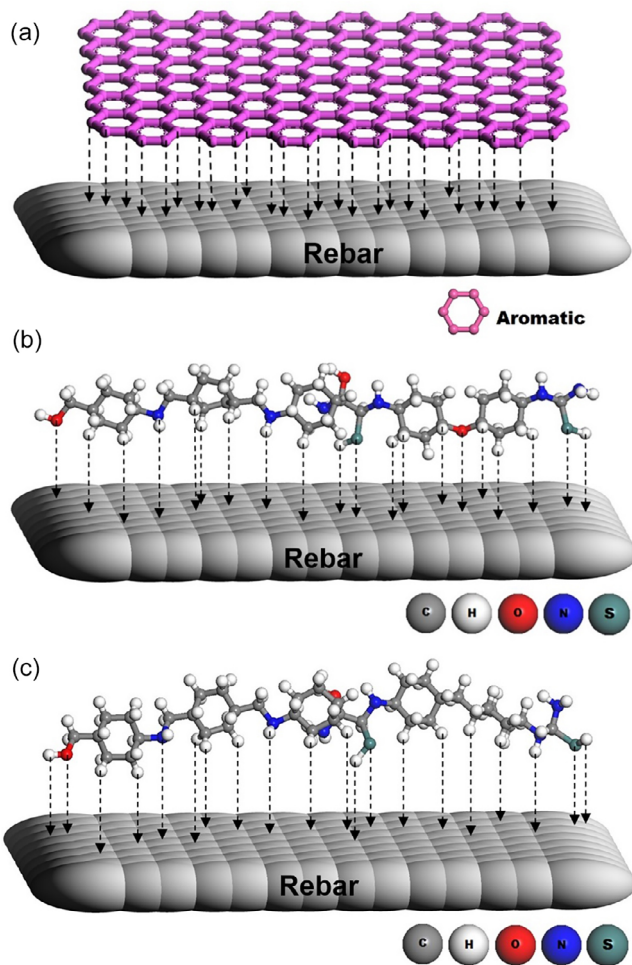


Figure 9. Mechanism of inhibition through a) adsorption of aromatic ring present in the polymers on metal (steel rebar) sites b) adsorption of PAMA1 polymer on steel surface and c) adsorption of PAMA2 polymer on steel surface.

99.62% was obtained by the PAMA1 at 1000 ppm concentration for the protection of the steel rebar from corrosion. Also, results indicate that appreciable and remarkable inhibition efficiencies of the inhibitors towards the corrosion protection of rebar have been achieved at low concentration level itself. SEM and AFM studies support the formation of protective layer on the surface of the rebar by the polymeric inhibitors during corrosion. Further, inhibition mechanism by the polyamide inhibitors for the corrosion protection of rebar in presence of chloride ions has been explained based on the possible interaction between the functional groups of the polymers with the rebar surface. Hence, the present study concludes the emergence of polymeric inhibitors towards the corrosion protection of steel rebar under vulnerable chloride rich environments.

Notes

The authors declare no competing financial interests.

Acknowledgements

Authors gratefully acknowledge the constant encouragement and support received from the Indian Institute of Technology Kanpur, CSIR – Structural Engineering Research Centre, Chennai and Bharathiar University, Coimbatore, India. B.B acknowledges the help provided by Dr. G.

Sathyan, NPDF, IIT Kanpur, during the preparation of the manuscript.

References

- [1] Zhang F, Ju P, Pan M, Zhang D, Huang Y, Li G, et al. Self-healing mechanisms in smart protective coatings: A review. *Corrosion Science* 2018;144:74-88. doi:[10.1016/j.corsci.2018.08.005](https://doi.org/10.1016/j.corsci.2018.08.005)
- [2] Li X, Zhang D, Liu Z, Li Z, Du C, Dong C. Materials science: share corrosion data. *Nature News* 2015;527:441. doi:[10.1038/527441a](https://doi.org/10.1038/527441a)
- [3] Chang C-H, Huang T-C, Peng C-W, Yeh T-C, Lu H-I, Hung W-I, et al. Novel anticorrosion coatings prepared from polyaniline/graphene composites. *Carbon* 2012;50:5044-51. doi:[10.1016/j.carbon.2012.06.043](https://doi.org/10.1016/j.carbon.2012.06.043)
- [4] Wei H, Ding D, Wei S, Guo Z. Anticorrosive conductive polyurethane multiwalled carbon nanotube nanocomposites. *Journal of Materials Chemistry A* 2013;1:10805-13. doi:[10.1039/c3ta11966a](https://doi.org/10.1039/c3ta11966a)
- [5] Volpi E, Foadelli C, Trasatti S, Koleva DA. Development of Smart Corrosion Inhibitors for Reinforced Concrete Structures Exposed to a Microbial Environment. *Industrial & Engineering Chemistry Research* 2017;56:5778-94. doi:[10.1021/acs.iecr.7b00127](https://doi.org/10.1021/acs.iecr.7b00127)
- [6] Selvaraj R, Bhuvaneshwari B. Characterization and development of organic coatings for steel rebars in concrete. *Portugaliae Electrochimica Acta* 2009;27:657-70. doi:[10.4152/pea.200906657](https://doi.org/10.4152/pea.200906657)
- [7] Ramesh S, Bhuvaneshwari B, Palani GS, Lal DM, Iyer NR. Effects on corrosion resistance of rebar subjected to deep cryogenic treatment. *Journal of Mechanical Science and Technology* 2017;31:123-32. doi:[10.1007/s12206-016-1211-5](https://doi.org/10.1007/s12206-016-1211-5)
- [8] Bhuvaneshwari B, Selvaraj A, Iyer NR, Ravikumar L. Electrochemical investigations on the performance of newly synthesized azomethine polyester on rebar corrosion. *Materials and Corrosion* 2015;66:387-95. doi:[10.1002/maco.201307472](https://doi.org/10.1002/maco.201307472)
- [9] Ramesh S, Bhuvaneshwari B, Palani GS, Mohan Lal D, Mondal K, Gupta RK. Enhancing the corrosion resistance performance of structural steel via a novel deep cryogenic treatment process. *Vacuum* 2019;159:468-75. doi:[10.1016/j.vacuum.2018.10.080](https://doi.org/10.1016/j.vacuum.2018.10.080)
- [10] Söylev TA, Richardson MG. Corrosion inhibitors for steel in concrete: State-of-the-art report. *Construction and Building Materials* 2008;22:609-22. doi:[10.1016/j.conbuildmat.2006.10.013](https://doi.org/10.1016/j.conbuildmat.2006.10.013)
- [11] Elsener B, Angst U. 14 - Corrosion inhibitors for reinforced concrete. In: Aitcin P-C, Flatt RJ, editors. *Science and Technology of Concrete Admixtures*: Woodhead Publishing 2016. p. 321-39.
- [12] Bellezze T, Timofeeva D, Giuliani G, Roventi G. Effect of soluble inhibitors on the corrosion behaviour of galvanized steel in fresh concrete. *Cement and Concrete Research* 2018;107:1-10. doi:[10.1016/j.cemconres.2018.02.008](https://doi.org/10.1016/j.cemconres.2018.02.008)
- [13] Jung MS, Kim KB, Lee SA, Ann KY. Risk of chloride-induced corrosion of steel in SF concrete exposed to a chloride-bearing environment. *Construction and Building Materials* 2018;166:413-22. doi:[10.1016/j.conbuildmat.2018.01.168](https://doi.org/10.1016/j.conbuildmat.2018.01.168)
- [14] Dong B, Ding W, Qin S, Han N, Fang G, Liu Y, et al. Chemical self-healing system with novel microcapsules for corrosion inhibition of rebar in concrete. *Cement and Concrete Composites* 2018;85:83-91. doi:[10.1016/j.cemconcomp.2017.09.012](https://doi.org/10.1016/j.cemconcomp.2017.09.012)
- [15] Jiang S, Jiang L, Wang Z, Jin M, Bai S, Song S, et al. Deoxyribonucleic acid as an inhibitor for chloride-induced corrosion of reinforcing steel in simulated concrete pore solutions. *Construction and Building Materials* 2017;150:238-47. doi:[10.1016/j.conbuildmat.2017.05.157](https://doi.org/10.1016/j.conbuildmat.2017.05.157)

- [16] Verbruggen H, Terryn H, De Graeve I. Inhibitor evaluation in different simulated concrete pore solution for the protection of steel rebars. *Construction and Building Materials* 2016;124:887-96. doi:10.1016/j.conbuildmat.2016.07.115
- [17] Valcarce M, López C, Vázquez M. The role of chloride, nitrite and carbonate ions on carbon steel passivity studied in simulating concrete pore solutions. *Journal of the Electrochemical Society* 2012;159:C244-C51. doi:10.1149/2.006206jes
- [18] Królikowski A, Kuziak J. Impedance study on calcium nitrite as a penetrating corrosion inhibitor for steel in concrete. *Electrochimica Acta* 2011;56:7845-53. doi:10.1016/j.electacta.2011.01.069
- [19] Fei F-l, Hu J, Wei J-x, Yu Q-j, Chen Z-s. Corrosion performance of steel reinforcement in simulated concrete pore solutions in the presence of imidazoline quaternary ammonium salt corrosion inhibitor. *Construction and Building Materials* 2014;70:43-53. doi:10.1016/j.conbuildmat.2014.07.082
- [20] Jiang S, Gao S, Jiang L, Guo M-Z, Jiang Y, Chen C, et al. Effects of Deoxyribonucleic acid on cement paste properties and chloride-induced corrosion of reinforcing steel in cement mortars. *Cement and Concrete Composites* 2018;91:87-96. doi:10.1016/j.cemconcomp.2018.05.002
- [21] Lee H-S, Yang H-M, Singh JK, Prasad SK, Yoo B. Corrosion mitigation of steel rebars in chloride contaminated concrete pore solution using inhibitor: An electrochemical investigation. *Construction and Building Materials* 2018;173:443-51. doi:10.1016/j.conbuildmat.2018.04.069
- [22] Wang Y, Zuo Y, Tang Y. Inhibition effect and mechanism of sodium oleate on passivation and pitting corrosion of steel in simulated concrete pore solution. *Construction and Building Materials* 2018;167:197-204. doi:10.1016/j.conbuildmat.2018.01.170
- [23] Diamanti MV, Pérez Rosales EA, Raffaini G, Ganazzoli F, Brenna A, Pedferri M, et al. Molecular modelling and electrochemical evaluation of organic inhibitors in concrete. *Corrosion Science* 2015;100:231-41. doi:10.1016/j.corsci.2015.07.034
- [24] Xu C, Jin WL, Wang HL, Wu HT, Huang N, Li ZY, et al. Organic corrosion inhibitor of triethylenetetramine into chloride contamination concrete by eletro-injection method. *Construction and Building Materials* 2016;115:602-17. doi:10.1016/j.conbuildmat.2016.04.076
- [25] Bastidas DM, Criado M, Fajardo S, La Iglesia A, Bastidas JM. Corrosion inhibition mechanism of phosphates for early-age reinforced mortar in the presence of chlorides. *Cement and Concrete Composites* 2015;61:1-6. doi:10.1016/j.cemconcomp.2015.04.009
- [26] Garcés P, Saura P, Méndez A, Zornoza E, Andrade C. Effect of nitrite in corrosion of reinforcing steel in neutral and acid solutions simulating the electrolytic environments of micropores of concrete in the propagation period. *Corrosion Science* 2008;50:498-509. doi:10.1016/j.corsci.2007.08.016
- [27] Bryan NS, Alexander DD, Coughlin JR, Milkowski AL, Boffetta P. Ingested nitrate and nitrite and stomach cancer risk: An updated review. *Food and Chemical Toxicology* 2012;50:3646-65. doi:10.1016/j.fct.2012.07.062
- [28] Fares MM, Maayta AK, Al-Mustafa JA. Corrosion inhibition of iota-carrageenan natural polymer on aluminum in presence of zwitterion mediator in HCl media. *Corrosion Science* 2012;65:223-30. doi:10.1016/j.corsci.2012.08.018
- [29] Biswas A, Pal S, Udayabhanu G. Experimental and theoretical studies of xanthan gum and its graft co-polymer as corrosion inhibitor for mild steel in 15% HCl. *Applied Surface Science* 2015;353:173-83. doi:10.1016/j.apsusc.2015.06.128
- [30] Pereira da Silva JE, Córdoba de Torresi SI, Torresi RM. Polyaniline acrylic coatings for corrosion inhibition: the role played by counter-ions. *Corrosion Science* 2005;47:811-22. doi:10.1016/j.corsci.2004.07.014
- [31] da Silva JEP, de Torresi SIC, Torresi RM. Polyaniline/poly(methylmethacrylate) blends for corrosion protection: The effect of passivating dopants on different metals. *Progress in Organic Coatings* 2007;58:33-9. doi:10.1016/j.porgcoat.2006.11.005
- [32] Andreeva DV, Skorb EV, Shchukin DG. Layer-by-Layer Polyelectrolyte/Inhibitor Nanostructures for Metal Corrosion Protection. *ACS Appl Mater Interfaces* 2010;2:1954-62. doi:10.1021/am1002712
- [33] Salem AA, Grgur BN. The influence of the polyaniline initial oxidation states on the corrosion of steel with composite coatings. *Progress in Organic Coatings* 2018;119:138-44. doi:10.1016/j.porgcoat.2018.02.032
- [34] Ramezanzadeh B, Bahlakeh G, Ramezanzadeh M. Polyaniline-cerium oxide (PAni-CeO₂) coated graphene oxide for enhancement of epoxy coating corrosion protection performance on mild steel. *Corrosion Science* 2018;137:111-26. doi:10.1016/j.corsci.2018.03.038
- [35] Ramezanzadeh B, Mohamadzadeh Moghadam MH, Shohani N, Mahdavian M. Effects of highly crystalline and conductive polyaniline/graphene oxide composites on the corrosion protection performance of a zinc-rich epoxy coating. *Chemical Engineering Journal* 2017;320:363-75. doi:10.1016/j.cej.2017.03.061
- [36] Grgur BN, Elkais AR, Gvozdenović MM, Drmanić SŽ, Trišović TL, Jugović BZ. Corrosion of mild steel with composite polyaniline coatings using different formulations. *Progress in Organic Coatings* 2015;79:17-24. doi:10.1016/j.porgcoat.2014.10.013
- [37] Sababi M, Pan J, Augustsson P-E, Sundell P-E, Claesson PM. Influence of polyaniline and ceria nanoparticle additives on corrosion protection of a UV-cure coating on carbon steel. *Corrosion Science* 2014;84:189-97. doi:10.1016/j.corsci.2014.03.031
- [38] Hu J, Koleva DA, Petrov P, van Breugel K. Polymeric vesicles for corrosion control in reinforced mortar: Electrochemical behavior, steel surface analysis and bulk matrix properties. *Corrosion Science* 2012;65:414-30. doi:10.1016/j.corsci.2012.08.043
- [39] Basha Nusrath Unnisa C, Nirmala Devi G, Hemapriya V, Chitra S, Chung I-M, Kim S-H, et al. Linear polyesters as effective corrosion inhibitors for steel rebars in chloride induced alkaline medium – An electrochemical approach. *Construction and Building Materials* 2018;165:866-76. doi:10.1016/j.conbuildmat.2018.01.080
- [40] Murugesan A, Ravikumar L, SathyaSelvaBala V, Senthil-Kumar P, Vidhyadevi T, Kirupha SD, et al. Removal of Pb(II), Cu(II) and Cd(II) ions from aqueous solution using polyazomethineamides: Equilibrium and kinetic approach. *Desalination* 2011;271:199-208. doi:10.1016/j.desal.2010.12.029
- [41] Ravikumar L, Kalaivani S, Vidhyadevi T, Murugasan A, Kirupha SD, Sivanesan S. Synthesis, Characterization and Metal Ion Adsorption Studies on Novel Aromatic Poly(Azomethine Amide)s Containing Thiourea Groups. *Open Journal of Polymer Chemistry* 2014;04(01):1-11. doi:10.4236/ojpcchem.2014.41001
- [42] Practice for Calculation of Corrosion Rates and Related Information from Electrochemical Measurements. *ASTM International*; doi:10.1520/g0102
- [43] Mansfeld F, Kendig MW, Tsai S. Recording and Analysis of AC Impedance Data for Corrosion Studies. *Corrosion* 1982;38:570-80. doi:10.5006/1.3577304
- [44] Sabirneeza AAF, Subhashini S, Rajalakshmi R. Water soluble conducting polymer composite of polyvinyl alcohol and leucine: An effective acid corrosion inhibitor for mild steel. *Materials and Corrosion* 2013;64:74-82. doi:10.1002/maco.201106096
- [45] Algabber AS, El-Nemma EM, Saleh MM. Effect of octylphe-

nol polyethylene oxide on the corrosion inhibition of steel in 0.5M H₂SO₄. Materials Chemistry and Physics 2004;86(1):26-32.
doi:[10.1016/j.matchemphys.2004.01.040](https://doi.org/10.1016/j.matchemphys.2004.01.040)

Open Access

This article is licensed under a [Creative Commons Attribution 4.0 International License](https://creativecommons.org/licenses/by/4.0/).

© The Author(s) 2018